scientific reports

Check for updates

OPEN

Sustainable plant mediated synthesis of cobalt oxide nanoparticles using *Uraria picta* extract with enhanced biological activity

S. Sheikh[1], A. J. Mungole[1]✉, Ajmal R. Bhat[2]✉, A. P. Pawar[3], C. P. Pandhurnekar[4], H. C. Pandhurnekar[5], Rizwan Wahab[6], H. P. Kanfade[7], Vijay Jagdish Upadhye[8]✉, Sumeer Ahmed[9]✉, Dalesh M. Parshuramkar[10], Mohammad Al-Omari[11] & Palani Elumalai[12]

The present study demonstrates a sustainable phytogenic route for the synthesis of cobalt oxide nanoparticles (CoO NPs) utilizing Uraria picta (Jacq.) DC. plant extract as a natural reducing and stabilizing agent. The whole plant was collected, shade-dried, powdered, and processed to obtain an aqueous extract, which was subsequently reacted with cobalt chloride hexahydrate stock solution, leading to the formation of CoO NPs *via* a green synthesis pathway. The appearance of a distinct color change confirmed nanoparticle formation. The resulting material was centrifuged, filtered, dried, and calcined to obtain blackish-violet CoO NPs. Comprehensive characterization of the biosynthesized nanoparticles was performed using UV–Vis spectroscopy, FTIR, XRD, EDS, SEM, and TEM analyses, confirming their structural, morphological, and elemental properties. Furthermore, the synthesized CoO NPs exhibited significant antioxidant potential and antibacterial activity against selected bacterial strains. This eco-friendly and cost-effective green synthesis approach not only avoids hazardous chemicals but also provides a promising strategy for the development of nanomaterials with potential biological and environmental applications.

Keywords Green synthesis, Cobalt oxide nanoparticles, Phytogenic synthesis, *Uraria picta* (Jacq.) DC., Biological applications

Nanoparticles are materials with dimensions ranging from 1 to 100 nm, exhibiting unique physico-chemical properties that differ significantly from their bulk counterparts. One of the most distinctive features of nanoparticles is their high surface-to-volume ratio which increases as particle size decreases, imparting remarkable optical, electrical and mechanical properties[1–4]. Owing to these properties, nanoparticles have been extensively utilized in diverse fields such as medical sciences[5–8], biomedical research[9,10], food packaging[11,12], textiles[13,14], water purification[15,16], construction[17–19], batteries[20–23], electronics[24–26], solar photovoltaics[27–31], fuel cells[32–34], sensors[35–38] and pharmaceutical applications, including anti-cancer therapeutics[39]. Metal

[1]Department of Botany, Nevjabai Hitkarini College, Bramhapuri 441 206, Maharashtra, India. [2]Department of Chemistry, RTM Nagpur University, Nagpur 440 033, India. [3]Department of Chemistry, Nevjabai Hitkarini College, Bramhapuri 441 206, Maharashtra, India. [4]Department of Chemistry, Shri Ramdeobaba College of Engineering and Management, Ramdeobaba University, Nagpur 440 013, Maharashtra, India. [5]Department of Chemistry, Dada Ramchand Bakhru Sindhu Mahavidyalaya, Nagpur 440 017, Maharashtra, India. [6]Department of Zoology, College of Science, King Saud University, Riyadh 11451, Saudi Arabia. [7]Department of Botany, Shantabai Mahila Mahavidyalaya, Bramhapuri 441 206, Maharashtra, India. [8]Deptartment of Microbiology, Parul Institute of Applied Sciences (PIAS), Parul University, PO, Limda, Tal Waghodia 391 760, India. [9]Natural Products and Medicinal Chemistry Division, CSIR - Indian Institute of Integrative Medicine, Jammu 180 001, India. [10]Department of Physics, Nevjabai Hitkarini College, Bramhapuri 441 206, Maharashtra, India. [11]Chemistry Department, Faculty of Science, Applied Science Private University, P.O. Box 166, Amman 11931, Jordan. [12]Department of Chemical Engineering and Biotechnology, University of Cambridge, Cambridge CB3 0AS, UK. ✉email: aru.mungole@gmail.com; bhatajmal@gmail.com; dr.vijaysemilo@gmail.com; sumeerchoudhary15@gmail.com

oxide nanoparticles, in particular, are of great interest due to their demonstrated antibacterial, antiviral, and antioxidant activities[36–41].

Conventionally, nanoparticles are synthesized using physical and chemical methods; however, these approaches are often expensive, energy-intensive and associated with the use of toxic reagents that can generate hazardous byproducts. To overcome these limitations, biosynthetic methods have emerged as promising alternatives owing to their sustainability, cost-effectiveness, and eco-friendly nature[42–44]. Plant-mediated synthesis of nanoparticles offers a sustainable alternative to conventional chemical methods by eliminating toxic reagents, reducing energy input, and utilizing renewable biomolecules as natural reducing and stabilizing agents[45,46]. This eco-friendly route not only minimizes environmental burden but also enhances biocompatibility, aligning with principles of green chemistry and circular economy. Among the biological methods, plant extract-mediated synthesis is considered the most efficient, scalable and straightforward approach compared to bacterial or fungal-mediated routes. Plant-derived phytochemicals, including ketones, aldehydes, flavones, terpenoids, carboxylic acids, phenols, and ascorbic acid, play a vital role in nanoparticle synthesis by acting as reducing, stabilizing and capping agents, thereby preventing agglomeration of nanoparticles[47–49].

Cobalt oxide nanoparticles (CoO NPs) are multifunctionfigal materials, classified as antiferromagnetic p-type semiconductors and belong to the family of transition metal oxides[50–52]. They have been widely investigated for applications in Lithium-ion rechargeable batteries, energy storage devices, heterogeneous catalysis, electrochromic sensors, pigments and dyes[53–57]. Moreover, CoO NPs have shown significant potential as electrode materials in pseudo-capacitors[58]. In biomedical sciences, cobalt oxide nanoparticles have garnered attention due to their unique bioactivities, including anticancer properties, which are attributed to their enhanced cellular uptake and ability to induce apoptosis in cancer cells[59,60]. Notably, cobalt also serves as an essential component of vitamin B12, further underlining its physiological relevance[61].

Several studies have demonstrated the potential of plant-mediated synthesis of CoO NPs for biomedical applications. For instance, cobalt oxide nanoparticles synthesized using *Emblica officinalis* extract have been investigated for their role in anemia treatment due to their link with vitamin B12[62], while *Geranium wallichianum* extract-mediated CoO NPs exhibited antibacterial, antifungal, enzyme inhibition, biocompatibility and anticancer properties[63]. Similarly, CoO NPs synthesized from *Ziziphora clinopodioides* Lam showed cytotoxic, antioxidant, antifungal, antibacterial, and wound-healing activities, along with enzyme inhibition potential[64]. In another study, CoO NPs synthesized using *Vibrio* species demonstrated antitumor potential against colorectal cancer, highlighting their role as promising candidates in cancer nanomedicine[65].

The present study focuses on *Uraria picta* (Jacq.) DC., a perennial herb belonging to the family Leguminosae–Papilionaceae. This plant is widely distributed in tropical Africa, South and Southeast Asia, and Australia, typically growing in dry grasslands, sandy soils, and rocky habitats[66]. Traditionally, *Uraria picta* has been employed in Ayurvedic, Unani, and Chinese medicinal systems and is an important constituent of Dashmula, a classical Ayurvedic formulation comprising ten medicinal herbs[67]. The plant is reputed for its therapeutic properties, including antibacterial, antidiabetic, anticancer, and anti-inflammatory activities[68], attributed to its rich phytochemical profile consisting of flavonoids, isoflavones, triterpenes, phenolics, tannins, cardiac glycosides, saponins and steroids[69]. Previous research has suggested that plant-derived metabolites such as alkaloids and flavonoids are effective mediators for nanoparticle synthesis[70]. Despite the growing interest in plant-mediated synthesis of metal oxide nanoparticles, no studies have yet reported the synthesis of cobalt oxide nanoparticles using *Uraria picta* (Jacq.) DC. Therefore, this plant extract was selected for the present investigation (Fig. 1). In this study, we report for the first time the phytogenic synthesis of CoO NPs using *U. picta* extract. It is rich in flavonoids, phenolics, alkaloids, and glycosides. These diverse bioactive compounds act as efficient reducing and capping agents, enabling controlled CoO nanoparticle synthesis and highlighting its novelty in green nanotechnology[71]. The synthesized nanoparticles were subjected to comprehensive physicochemical characterization and their biological activities, including antioxidant and antibacterial potentials, were systematically evaluated.

Materials and methods

All chemicals and reagents used in the present study were of analytical grade and of the highest possible purity. Cobalt chloride hexahydrate ($CoCl_2{\cdot}6H_2O$, Purity: 98%) and butyl hydroxytoluene (BHT) were procured from Merck Chemicals, India. 1, 1-Diphenyl-2-picrylhydrazyl (DPPH) was obtained from Sigma-Aldrich, India. Organic solvents such as acetone, n-hexane, ethanol, and methanol were purchased from S. D. Fine Chemicals, India. Authenticated strain cultures were procured from Sai Biosystems Pvt. Ltd., Nagpur and ESONAWA Innovations Pvt. Ltd., Nagpur. The purity of each strain was confirmed based on colony characteristics on selective media: *E. coli* on Eosin Methylene Blue (EMB) agar, *B. subtilis* on Bacillus agar, *S. typhi* on Salmonella–Shigella (SS) agar, and *P. vulgaris* on Heart Infusion agar.

Plant collection and authentication

Uraria picta (Jacq.) DC., a perennial herb of the family Fabaceae, was selected for the present study. Fresh plant material was collected by Ms. S. Sheikh from Bramhapuri Tehsil, Chandrapur, District, Maharashtra, India (**Latitude: 20.62298° N**, **Longitude: 79.855588° E**). Prior permission for collection was obtained from the concerned Forest Department/competent authority, and the process was carried out in accordance with institutional, national, and international guidelines for the collection of plant material. The taxonomic identification and authentication of the species were carried out by the Department of Botany, Anand Niketan College, Warora, Dist. Chandrapur, Maharashtra, India, and a voucher specimen was deposited (Ref. No. ANC/Bot/2024/01/25BH) **Fig. S1-S3**. The collected material was carefully shade-dried to preserve its phytoconstituents, ground into a fine powder using a mortar and pestle, and stored in airtight containers until further use.

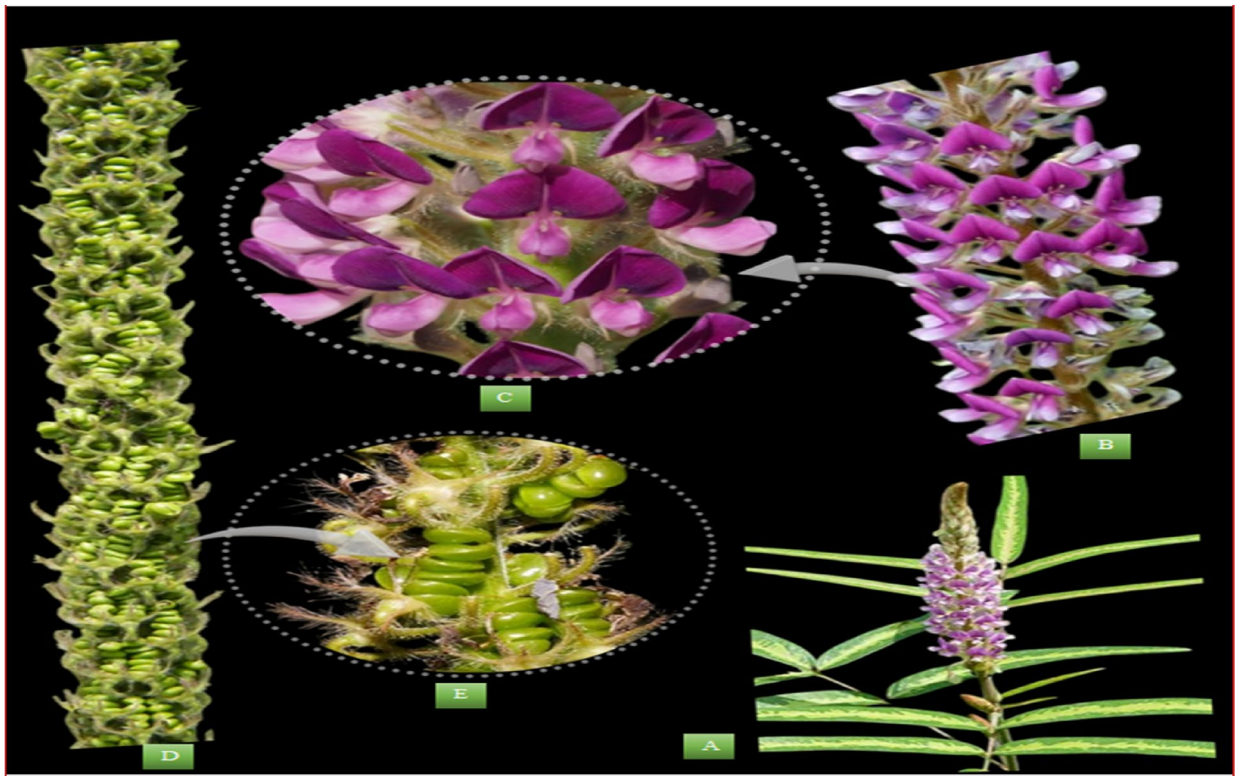

Fig. 1. *Uraria picta* (Jacq.) DC: (**A**) Habit (**B**) Inflorescence (**C**) Individual Flower (**D**) Fruits (**E**) Individual Fruit.

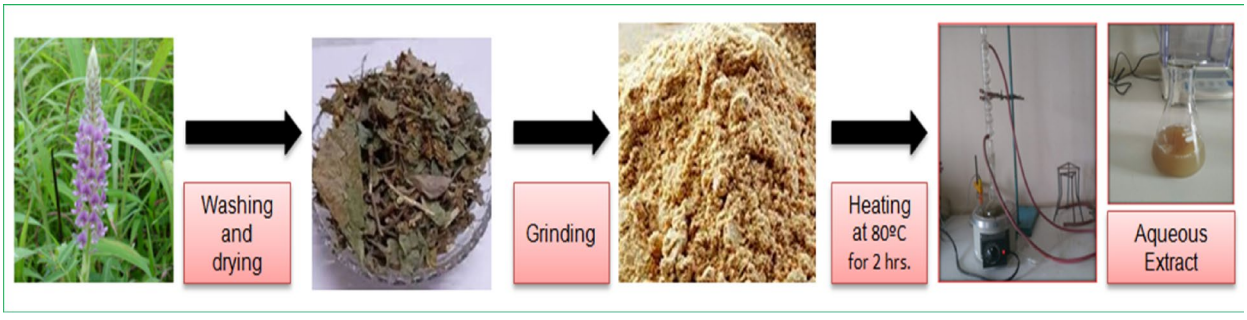

Fig. 2. Graphical representation of the preparation of the plant extract.

Preparation of plant extract

The whole plant of *Uraria picta* (Jacq.) DC. was collected from the forest region near Bramhapuri, Chandrapur district, Maharashtra, India. The freshly collected plant material was thoroughly washed with tap water to remove adhering dust and soil particles, followed by repeated washing with deionized distilled water at room temperature. The cleaned plant material was shade-dried completely, chopped into small pieces, and ground into a fine powder. For extract preparation, 25 g of the powdered material was transferred into a clean, dry round-bottom flask containing 250 mL of distilled water. The mixture was heated at 80 °C for 2 h on a heating mantle and subsequently cooled to room temperature. The cooled mixture was filtered using Whatman No. 41 filter paper, and the resulting filtrate was collected and stored at 0 °C for further experimental use Fig. 2[72].

Biosynthesis of Cobalt oxide nanoparticles (CoO NPs)

For the biosynthesis of CoO NPs, 100 mL of *Uraria picta* plant extract was taken in a 250 mL beaker, and 50 mL of cobalt chloride hexahydrate stock solution was added dropwise with continuous stirring. The mixture was maintained at 80 °C on a hot plate with constant stirring on the magnetic stirrer at 1200 rpm (Make: Remi, India) for 2 h to facilitate nanoparticle formation. After cooling to room temperature (27 °C), the reaction mixture was centrifuged at 10,000 rpm for 10 min to collect the pellet, while the supernatant was discarded. The obtained pellet was washed three times with deionized water to remove impurities, dried at 100 °C for 2

h, and subsequently calcined in furnace with gradual rise in the temperature of sample up to 500 °C and kept at constant temperature of 500 °C for 2 h to yield black-violet, highly crystalline cobalt oxide nanoparticles as depicted in the Fig. 3[72].

Characterization

The biosynthesized cobalt oxide nanoparticles were subjected to comprehensive characterization using advanced spectroscopic and microscopic techniques, including UV–Visible spectroscopy, Fourier-transform infrared

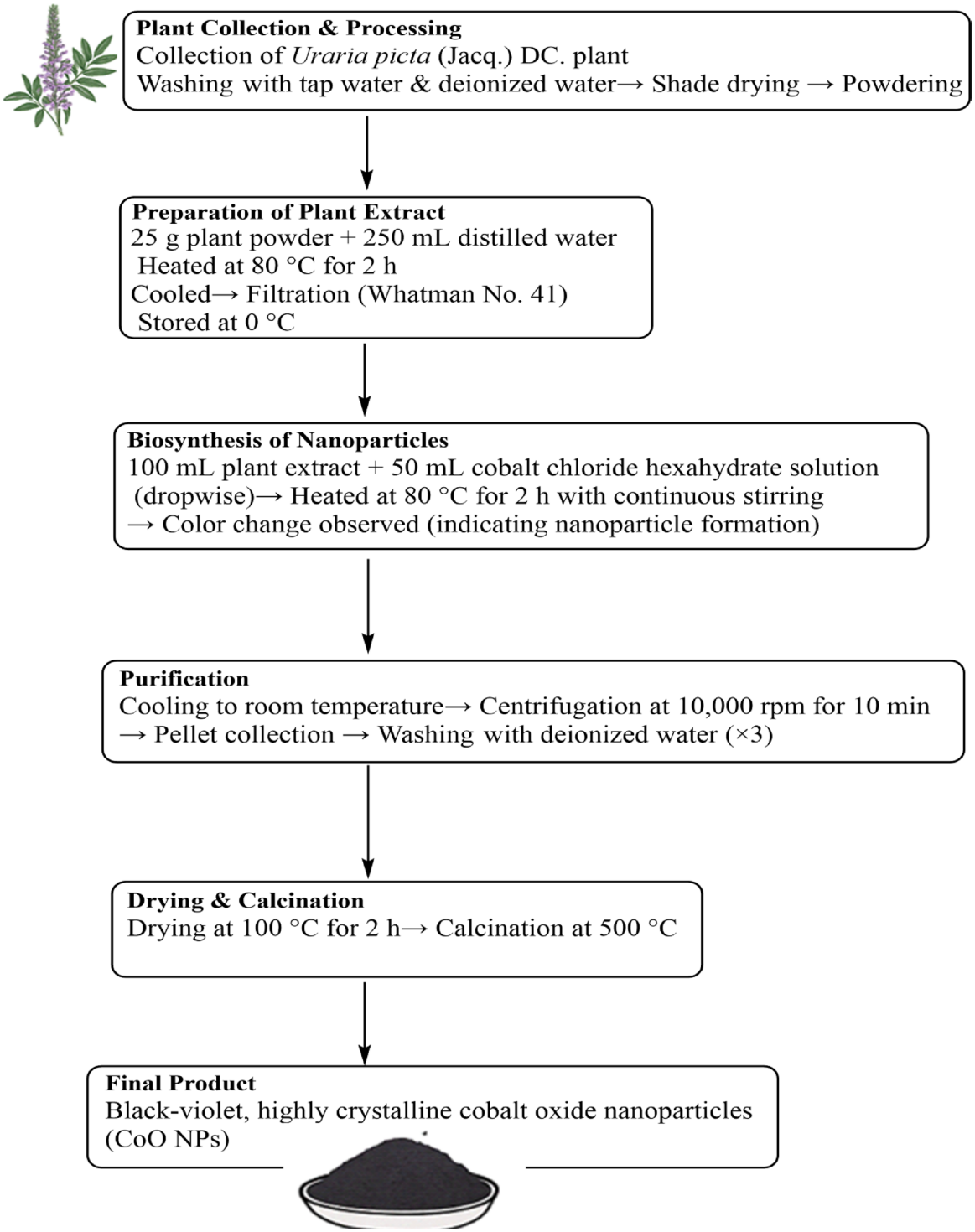

Fig. 3. Schematic Representation of Green Synthesis of Cobalt Oxide Nanoparticles (CoO NPs) Using *Uraria picta* Extract.

(FTIR) spectroscopy, powder X-ray diffraction (PXRD), scanning electron microscopy (SEM), transmission electron microscopy (TEM), and energy-dispersive X-ray analysis (EDAX/EDX).

The optical properties were examined using a UV–Visible spectrophotometer (EQUIPTRONICS, Model EQ-826) within the wavelength range of 190–1100 nm to investigate the absorbance behavior of the nanoparticles[73,74]. FTIR spectra were recorded using a Thermo Nicolet iS50 spectrophotometer (resolution 0.2 cm^{-1}) in the range of 400–4000 cm^{-1} to identify phytochemicals responsible for nanoparticle synthesis and stabilization. For this purpose, 1–2 mg of powdered sample was homogenized with ~ 100 mg of spectroscopic-grade KBr, compressed under 8–12 tonnes pressure into transparent pellets, and analyzed with an average of 64 scans per sample[73].

The crystalline structure and average crystallite size were determined by PXRD using a Bruker D8 Advance A25 diffractometer operating at 40 mA and 40 kV in Bragg–Brentano geometry. Samples were mounted on amorphous silica low-background holders for analysis[75]. Surface morphology and particle size distribution were observed via SEM (JEOL JSM-6390LV, Tokyo, Japan) at 15 kV. Samples were immobilized on carbon adhesive tape, sputter-coated with a thin gold layer using a JFC-1600 ion-sputtering device, and examined under varying magnifications to assess shape, surface topography, and aggregation behavior[76].

Elemental composition was investigated using EDX (Oxford XMX N system coupled with SEM). The technique allowed semi-quantitative detection of constituent elements with a sensitivity of approximately 0.5–1.0 wt%, enabling confirmation of nanoparticle purity and the presence of trace elements[77]. TEM analysis was performed using a JEOL JM-2100 microscope equipped with a Gatan imaging system to examine particle morphology, lattice fringes, and nanoscale features. For this analysis, nanoparticles were ultrasonically dispersed in ethanol, and a drop of the suspension was placed on a 200-mesh carbon-coated copper grid, air-dried, and mounted for imaging[78]. All analyses were carried out at the Sophisticated Analytical Instrumentation Facility (SAIF), Kochi, India.

Antibacterial activity of nanoparticles

Stock solution of nanoparticles

The biosynthesized nanoparticles were obtained in dried powdered form, as described in the synthesis protocol. For antibacterial screening against selected human pathogenic bacteria, a working stock solution was prepared by dispersing the nanoparticle powder in Dimethyl Sulfoxide (DMSO) at a concentration of 1 mg/mL. DMSO was chosen as the solvent due to its non-reactive nature toward most microbial species and its ability to enhance nanoparticle solubility.Prior to use in antibacterial assays, the nanoparticle suspensions were subjected to sonication to achieve uniform dispersion. Sonication was performed using a Labline 1.5 L water bath sonicator, wherein centrifuge tubes containing the nanoparticle suspension were immersed and treated for 15 min. The sonicated solutions were immediately utilized for antibacterial activity assays to minimize re-aggregation and ensure stability of the nanoparticle dispersion.

Procurement and maintenance of bacterial cultures

Four clinically relevant human pathogenic bacteria, namely *Escherichia coli* (*E. coli*), *Bacillus subtilis* (*B. subtilis*), *Salmonella typhi* (*S. typhi*) and *Proteus vulgaris* (*P. vulgaris*), were selected to evaluate the antibacterial potential of the synthesized nanoparticles. Antibacterial assays were conducted at three different nanoparticle concentrations, with gentamicin employed as the standard reference antibiotic and DMSO serving as the solvent control.

Inoculum Preparation for antibacterial assay

In the present study, *E. coli*, *B. subtilis*, *S. typhi*, and *P. vulgaris* were regularly maintained on their respective selective media and subsequently employed for antibacterial assays. For inoculum preparation, a loopful of each pure culture was transferred into 10 mL of sterile nutrient broth and incubated at 37 °C for 24 h. The bacterial suspensions were adjusted to match the 0.5 McFarland standard (equivalent to 1.0 O.D. at 600 nm), ensuring uniform turbidity prior to use in antibacterial testing.

Well diffusion assay for nanoparticles based antibacterial activity

Cobalt oxide nanoparticles were prepared at a stock concentration of 1 mg/mL and evaluated for their antibacterial activity against four human pathogenic bacteria, namely *E. coli*, *B. subtilis*, *S. typhi*, and *P. vulgaris* following standard procedures[79]. The in vitro antibacterial potential of the nanoparticles was assessed using Mueller–Hinton agar (MHA) and established microbiological techniques.

Antibacterial activity assay

Mueller–Hinton agar was prepared by dissolving 38 g of agar powder in 1000 mL of purified water. The mixture was boiled until completely dissolved and subsequently sterilized by autoclaving. After cooling to 45–50 °C, the medium was aseptically poured into sterile Petri plates and allowed to solidify. Each plate was inoculated with 10 µL of standardized bacterial broth culture using the pour-plate technique, followed by uniform spreading with a sterile spreader. Sterile steel borers were used to prepare equidistant wells in the solidified agar. The wells were filled with 25, 50, and 100 µL of nanoparticle suspensions, corresponding to 25, 50, and 100 µg/mL, respectively. Gentamicin was used as the positive control (disk diffusion method), while DMSO served as the negative control (well diffusion method). The plates were incubated at 37 °C for 24 h, and the zones of inhibition (mm) were measured to evaluate antibacterial activity.

Antioxidant activity of nanoparticles by DPPH assay

Working principle of DPPH assay

The DPPH assay was performed following the established protocol for stable free radical scavenging activity[80]. In this method, the DPPH radical, containing an unpaired electron, exhibits a maximum absorption at 517 nm, producing a characteristic purple color. When antioxidants are present, they donate hydrogen atoms to the DPPH radical, reducing it to its non-radical form (DPPH-H). This reduction leads to a decrease in absorbance at 517 nm[81]. The color change from purple to yellow, known as decolorization, reflects the extent of radical scavenging. A greater degree of decolorization corresponds to a higher number of electrons or hydrogen atoms donated by the antioxidants, thereby indicating stronger reducing potential[82].

Methodology

The DPPH (2,2-diphenyl-1-picrylhydrazyl) radical scavenging assay was performed using ascorbic acid as the standard reference antioxidant, following a modified protocol[83]. All test samples were evaluated alongside ascorbic acid. A 0.135 mM DPPH solution was prepared in methanol, and different concentrations of the test samples like 5, 10, 20, 40, 80, 160, and 320 µg/mL were prepared. Each concentration (2.5 mL) was mixed with the DPPH solution, vortexed thoroughly, and incubated at room temperature for 30 min in the dark. The absorbance was then measured at 517 nm using a UV–Vis spectrophotometer.

The free radical scavenging activity (%) was calculated using the following equation:

$$\%\ \text{DPPH scavenging} = \frac{(OD_{\text{control}} - OD_{\text{sample}})}{OD_{\text{contrao}}} \times 100$$

Where, OD (control) is the absorbance of the control (DPPH solution without sample) and OD (sample) is the absorbance in the presence of the test sample.

Results and discussion

The aqueous extract of *Uraria picta* has been utilized for the phytogenic synthesis of cobalt oxide nanoparticles (CoO NPs). Upon the drop wise addition of cobalt chloride hexahydrate solution to the plant extract under the condition of constant stirring and heating, a distinct color change was observed, signifying the reduction of Co^{2+} ions and the onset of nanoparticle formation. Following centrifugation, washing, drying, and calcination at 500 °C, a black-violet crystalline powder was obtained, confirming the successful synthesis of CoO NPs (Scheme 1).

The biomolecules such as flavonoids, phenolics, and alkaloids, present in the *Uraria picta* extract likely acted as both reducing and stabilizing agents, enabling the formation of nanoparticles without the involvement of toxic chemicals. This green approach not only ensured the eco-friendly and cost-effective synthesis of cobalt oxide but also highlighted the potential role of plant metabolites in nanoparticle stabilization. The crystalline nature of the final product is in agreement with earlier reports on biosynthesized metal oxide nanoparticles.

Spectral characterization of Cobalt oxide nanoparticles

The UV–Vis spectrum of *Uraria picta* mediated cobalt oxide nanoparticles exhibited a strong absorption maximum at ~ **300 nm**, with a smaller secondary peak near ~ **240 nm** (**Fig. S4**). These features likely arise from electronic transitions within the cobalt–oxygen framework and may reflect the presence of multiple cobalt oxidation states or a distribution of particle sizes. A comparable absorption band at 309 nm was reported for CoO NPs synthesized using *Coriandrum sativum* seed extract, supporting the assignment of this band to cobalt oxide-related transitions[84] and for *Allium sativum* at ~ 314 nm, *Hibiscus rosa-sinensis* derived Co_3O_4 NPs display a strong UV feature near 210 nm respectively[85,86]. The slight hypsochromic (blue) shift observed here suggests the formation of relatively smaller nanoparticles, consistent with quantum- or size-dependent spectral shifts. The prominent band also corresponds to charge-transfer/metal–oxygen electronic transitions commonly observed for cobalt oxides rather than true localized surface plasmon resonance. UV–Vis scans performed over 200–1100 nm (absorbance ≤ 1.5 OD) confirmed nanoparticle formation and showed no additional broad

1. **Reduction Step**

   The phytochemicals present in *Uraria picta* (such as phenolics, flavonoids, tannins, etc.) act as reducing agents, donating electrons and protons to cobalt ions:

   $CoCl_2.6H_2O \xrightarrow[\text{Plant extract (biomolecules)}]{} Co^{2+} + 2Cl^- + 6H_2O$

   $Co^{2+} + \text{Biomolecules}_{(red)} \longrightarrow Co^0 + \text{Biomolecules}_{(ox)}$

2. **Nucleation and Growth**

   The reduced cobalt atoms aggregate to form cobalt nanoparticles, stabilized by plant metabolites:

   $Co^0 \longrightarrow \text{Co (nanoclusters)} \longrightarrow \text{CO (NPs)}$

3. **Oxidation and Calcination**

   Upon calcination at 500 °C, cobalt nanoparticles oxidize to cobalt oxide nanoparticles:

   $2\text{CO (NPs)} + O_2 \longrightarrow \mathbf{2CoO\ (NPs)}$

Scheme 1. General Reaction Pattern for cobalt oxide nanoparticles.

plasmonic features, reinforcing that the recorded peaks are attributable to cobalt–oxygen electronic processes and size-dependent effects[87,88].

The FTIR spectrum of *Uraria picta*-mediated cobalt oxide nanoparticles revealed nine characteristic peaks at 3420.52, 3167.71, 2914.09, 2197.53, 1590.97, 1375.92, 1098.49, 912.17, and 611.76 cm^{-1} (Fig. 4). Compared to copper nanoparticles, CoO nanoparticles exhibited fewer peaks, suggesting relatively simpler vibrational modes. Interestingly, similar peak patterns were observed across different plant-mediated syntheses, confirming the role of phytochemicals as reducing and stabilizing agents during nanoparticle formation.

The broad absorption around 3420–3160 cm^{-1} corresponds to O–H stretching of hydroxyl groups and N–H stretching of amines, indicating the presence of phenolics and proteins from the extract. Peaks at ~ 2197 cm^{-1} are attributed to –OH stretching in phosphines, while the sharp band at ~ 1375 cm^{-1} is associated with C = O stretching of benzophenols and SO_2 vibrations. The band at ~ 1098 cm^{-1} corresponds to C–O/C–N stretching of aliphatic amines, and the peak at ~ 912 cm^{-1} is related to –C–O–C linkages. Importantly, the band at ~ 611 cm^{-1} represents Co–O stretching vibrations, confirming the formation of cobalt oxide nanoparticles. Similar FTIR features were reported for phyto-fabricated CoO NPs synthesized using *Psidium guajava* and other plant extracts, where strong O–H, N–H, C = O, and Co–O vibrations were observed[89–91]. These results collectively indicate that the functional groups from plant metabolites not only reduce cobalt ions but also cap and stabilize the nanoparticles, while the Co–O band validates the presence of crystalline cobalt oxide.

Scanning Electron Microscopy (SEM) of the green-synthesized CoO nanoparticles revealed irregular morphologies, predominantly ranging from roughly triangular to pyramidal shapes (Fig. 5). Such morphology is consistent with the influence of plant-derived phytochemicals, which act as capping and stabilizing agents during nanoparticle growth. Similar observations have been reported for CoO NPs synthesized using rosemary leaf extract, where semi-triangular to pyramidal particles with a wide size distribution were noted[92]. In contrast, CoO nanoparticles produced via *Fusarium oxysporum* exhibited polyshaped crystalline structures, and agglomeration was attributed to their magnetic induction properties[93]. The current SEM results confirm that the *Uraria picta* extract not only mediates nanoparticle formation but also influences particle shape and size, leading to irregular yet well-defined nanostructures suitable for various biological and catalytic applications.

Energy Dispersive Spectroscopy (EDS) was employed to determine the elemental composition of *Uraria picta*-mediated CoO nanoparticles, which exhibited a high cobalt content of 79.58 wt% and oxygen 20.42 wt% (Fig. 6). The spectrum showed two major peaks corresponding to cobalt and oxygen, confirming the formation of cobalt oxide, while minor peaks were attributed to residual phytochemicals from the plant extract acting as capping and stabilizing agents. These results are consistent with earlier studies, such as CoO NPs synthesized using *Alhagi maurorum*, where cobalt and oxygen dominated the composition[94], and *Euphorbia tirucalli*-mediated CoO nanoparticles, where minor peaks represented trace elements from plant metabolites, while cobalt oxide was the primary component[95]. The EDS analysis thus validates the successful green synthesis of CoO nanoparticles and highlights the role of plant biomolecules in stabilizing the nanostructures.

X-ray diffraction (XRD) was employed to investigate the crystalline structure of *Uraria picta*-mediated CoO nanoparticles, providing insights into their atomic-level organization, lattice parameters, and potential structural defects[96–98]. The XRD pattern (Fig. 7) displayed distinct diffraction peaks at 2θ = 37.36°, 42.95°, 43.84°, and

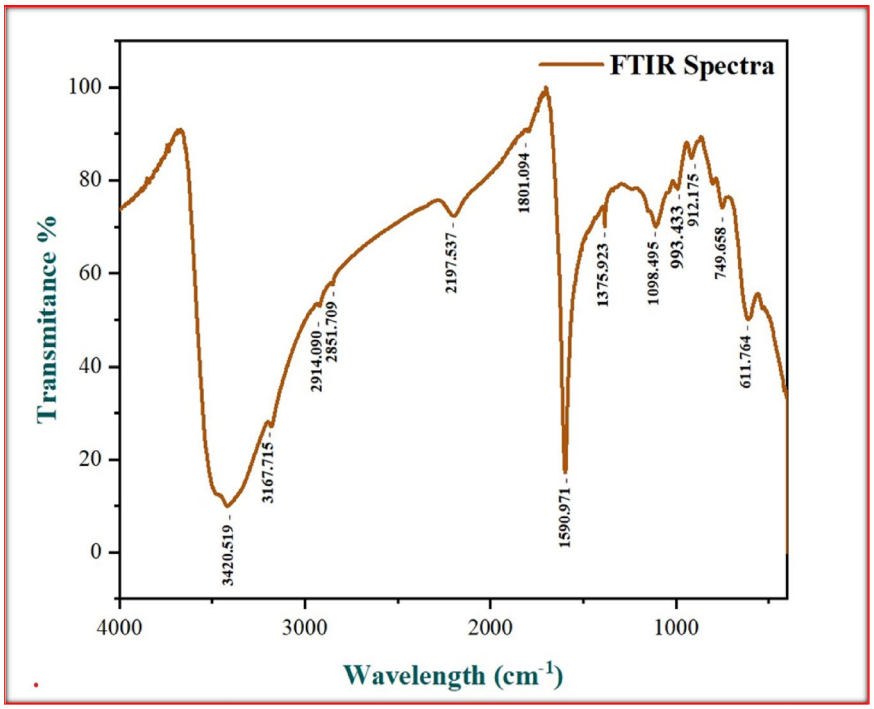

Fig. 4. *Uraria picta* based CoO NPs FTIR pattern.

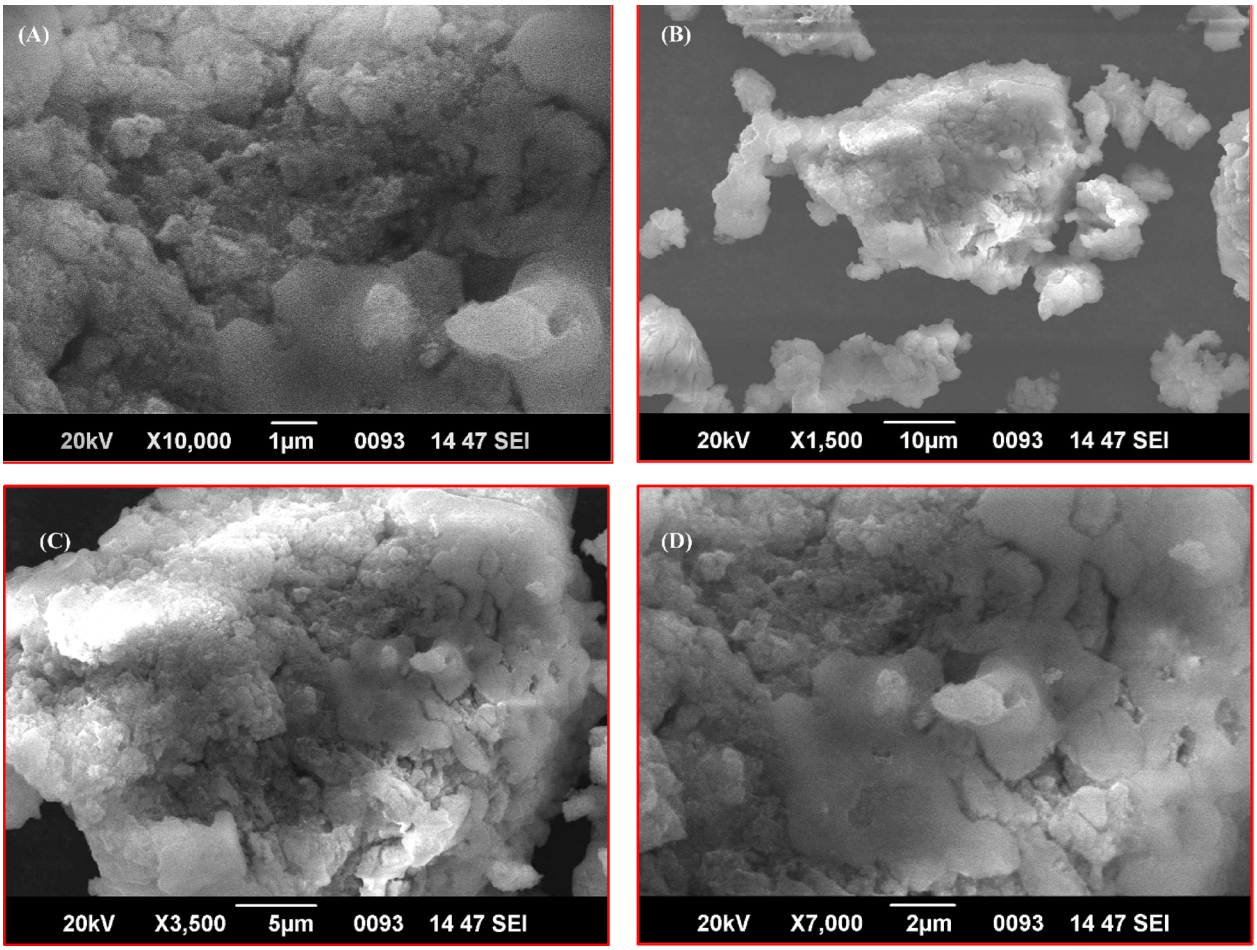

Fig. 5. (**A**) 20 kV X 10,000 resolution, (**B**) 20 kV X 1,500 resolution, (**C**) 20 kV X 3,500 resolution and (**D**) 20 kV X 7,000 resolution display SEM images of *Uraria picta-based* CoO NPs at low and high resolution.

61.87°, confirming the formation of highly crystalline cobalt oxide nanoparticles. The observed peaks correspond well with standard reference data from the International Centre for Diffraction Data (JCPDS card 96–152-8839). Comparable XRD patterns have been reported for CoO nanoparticles synthesized using *Pedalium murex* leaf extract, where well-defined peaks similarly indicated a crystalline structure[99]. The sharpness and intensity of the diffraction peaks in the present study suggest good crystallinity and uniform particle formation, consistent with the effective reduction and stabilization facilitated by phytochemicals in *Uraria picta*.

Cobalt oxide nanoparticles synthesized using *Uraria picta* extract exhibited a globular morphology with remarkably small dimensions (Fig. 8). Particle size analysis revealed an average diameter of 5.26 ± 0.74 nm, with a minimum size of 4.01 nm, a median of 5.40 nm, and a maximum of 6.27 nm, as summarized in Table 1. These findings indicate a narrow size distribution, consistent with the influence of plant-derived biomolecules in controlling nanoparticle growth and preventing excessive aggregation. Broadly, CoO NPs synthesized via green methods tend to exhibit sizes in the 4–5 nm range, highlighting the effectiveness of *Uraria picta* extract in producing uniform, ultra-small nanoparticles. The small size and globular morphology are expected to enhance the surface area and reactivity of the nanoparticles, making them suitable for various catalytic, biomedical, and electronic applications.

In a similar studies potential of Transmission Electron Microscope has been put forward to elucidate size of the NPs. CoO NPs with means size of 34 nm synthesized using *Hibisus rosa sinensis* flower extract able to control bacterial phytopathogens diseases investigated with Rice plants[100]. Cobalt oxide NPs synthesized from root of *Allium cepa* (onion bulb) found to be phytotoxic in nature also especially to plants via excessive absorption of cobalt oxide[101]. Thus, it in importance to screen the potential of such CoO NPs before getting commercialized especially of smaller size nanoparticles ranging between 10 and 15 nm. In a positive size CoO NPs found to be controlling cancer cell growth at 55 µg/mL concentration which was synthesized from plants and able to give sheet shaped cobalt oxide nanoparticles ranging between 15 and 20 nm[102].

Biological studies

Antimicrobial activity

The antibacterial activity of biosynthesized cobalt oxide nanoparticles (CoO NPs) was evaluated against four test bacterial strains (*E. coli* EC23, *B. subtilis* BS07, *S. typhi* ST12, and *P. vulgaris* PV05) using the agar well

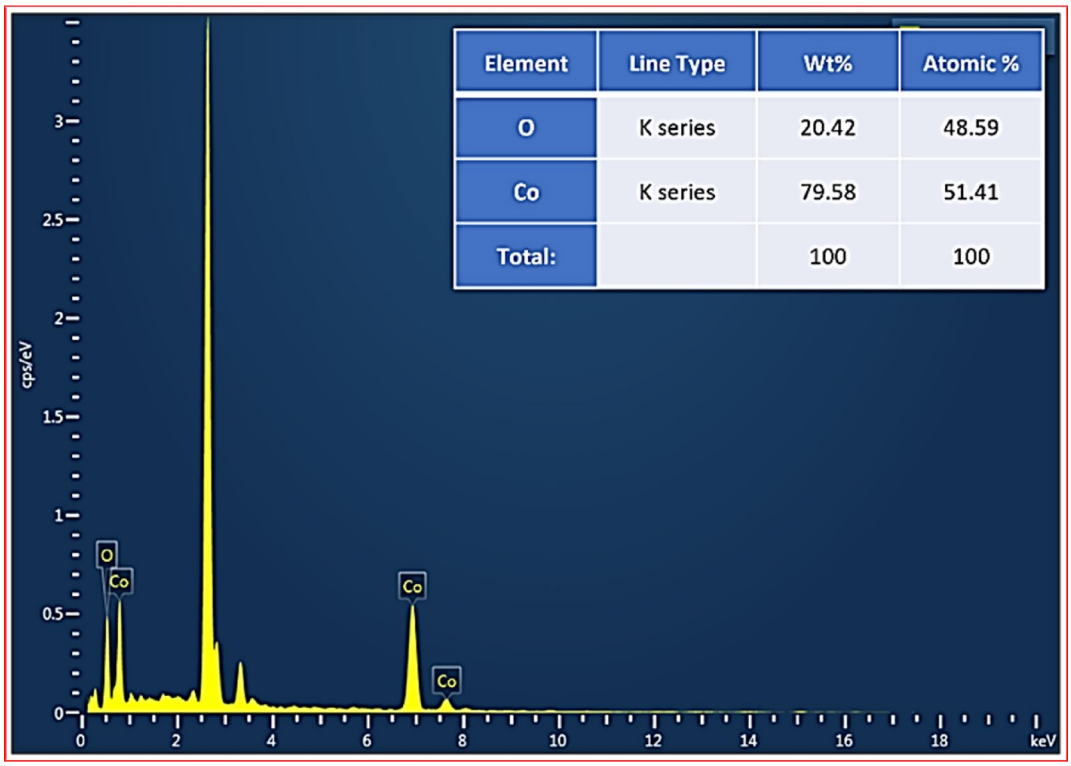

Fig. 6. EDS pattern of *Uraria picta* based CoO NPs.

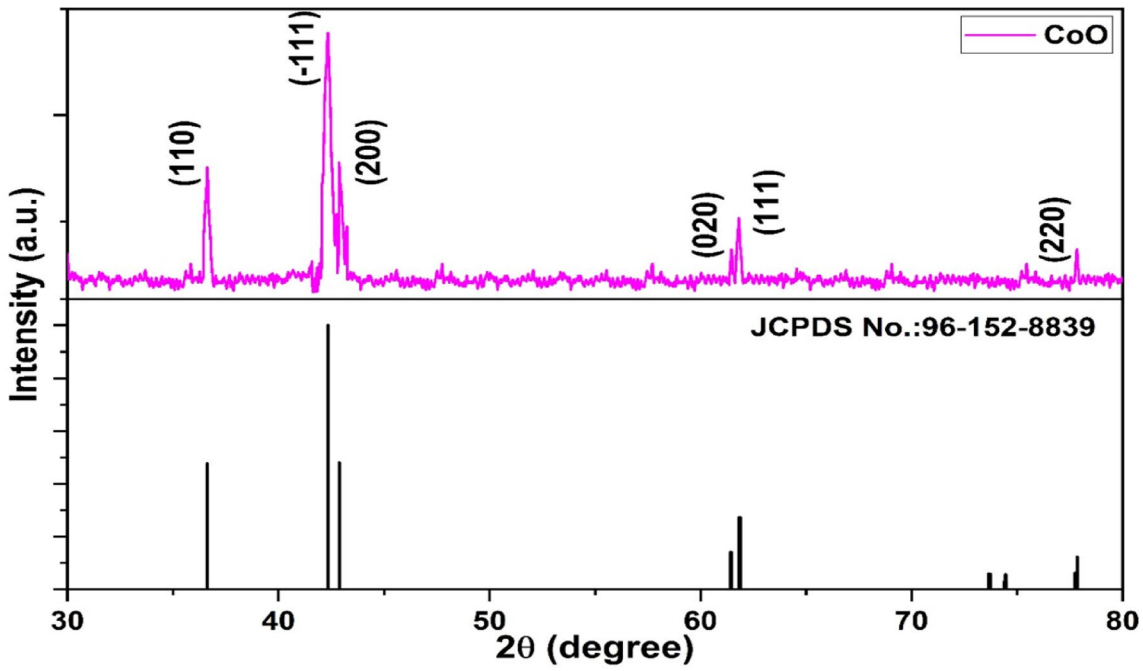

Fig. 7. XRD pattern of CoO NPs synthesised by using *Uraria picta*.

diffusion method[79], and the results were compared with the standard antibiotic gentamicin (120 µg/L). The zone of inhibition (ZOI) values revealed a clear concentration-dependent antibacterial effect of CoO NPs (Table 2 & **Fig. S5**). At the lowest concentration (25 µL), no inhibition was observed for any of the tested organisms, indicating that a threshold concentration of nanoparticles is necessary to elicit antibacterial action. However, at 50 µL, measurable inhibition zones appeared in all test strains, with maximum sensitivity shown by *B. subtilis*

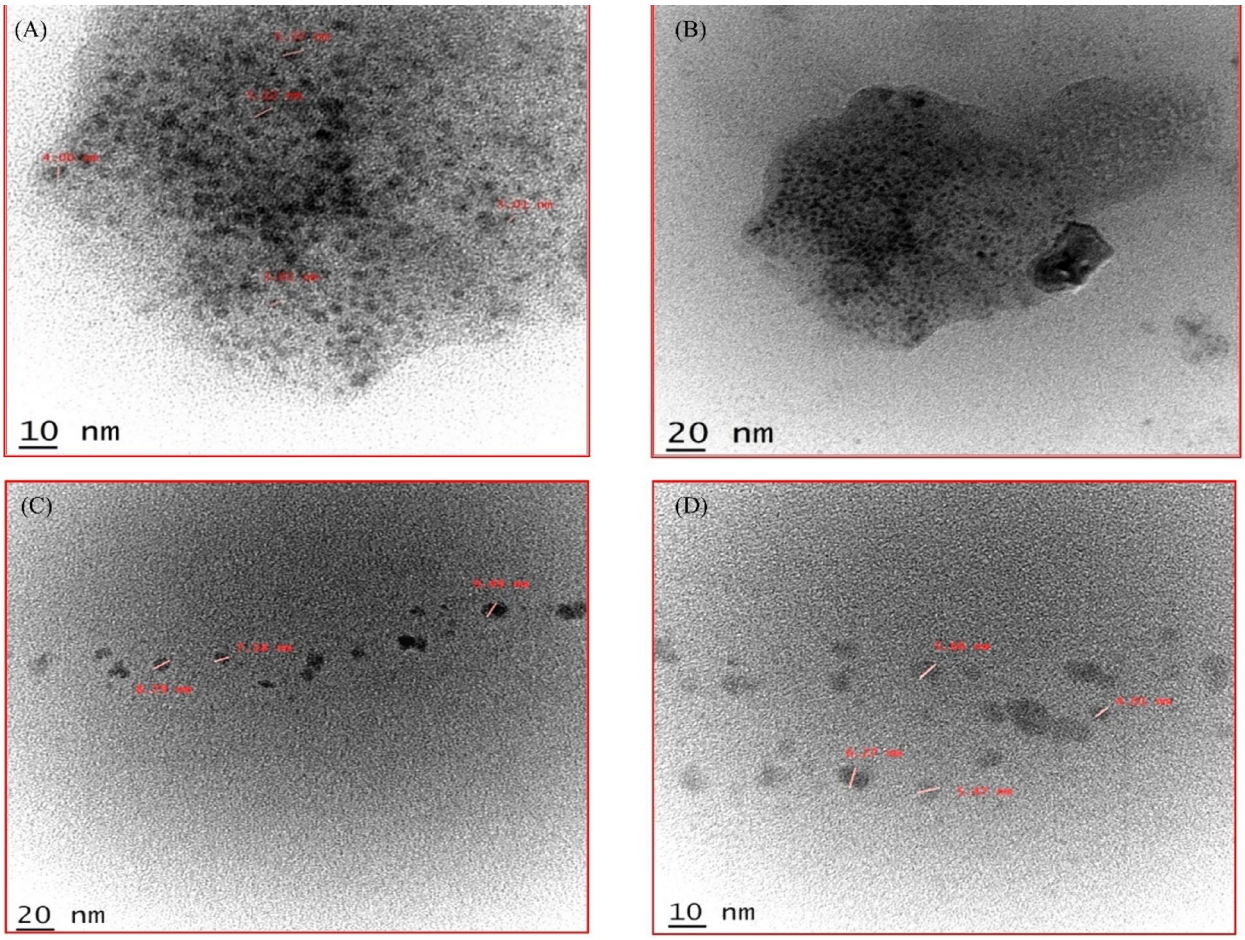

Fig. 8. Transmission Electron Micrograph of *Uraria picta* based CoO NPs (A) 10 nm resolution, (B) 20 nm resolution, (C) 20 nm resolution and (D) 10 nm resolution.

Minimum	**4.010 nm**
25% Percentile	4.775 nm
Median	5.395 nm
75% Percentile	5.798 nm
Maximum	6.270 nm
Mean ± Std deviation	**5.257** nm ± **0.7435** nm

Table 1. Average size of the CoO NPs recorded for the Minimum, Median, Maximum, Average, and standard Deviation.

	Zone of Inhibition in mm			
	Cobalt oxide nanoparticles (CoO NPs) Mean ± SD (mm)			
Test Organism	**25 µg/mL**	**50 µg/mL**	**100 µg/Ml**	**Zone of Inhibition in mm for Control (Gentamicin 120 µg/L) Mean ± SD**
EC23 (*E. coli*)	0.00 ± 0.00	13.67 ± 0.5774	17.33 ± 0.5774	23.57 ± 1.718
BS07 (*B. subtilis*)	0.00 ± 0.00	15.33 ± 0.5774	16.67 ± 0.5774	26.57 ± 2.370
ST12 (*S. typhi*)	0.00 ± 0.00	10.67 ± 0.5774	19.33 ± 1.155	21.86 ± 1.952
PV05 (*P. vulgaris*)	0.00 ± 0.00	12.00 ± 0.0	11.33 ± 0.5774	19.86 ± 1.952

Table 2. Anti-bacterial activity of CoO NPs at three concentrations along with standard drug against different bacterial strains.

(15.33 ± 0.57 mm), followed by *E. coli* (13.67 ± 0.57 mm), *P. vulgaris* (12.00 ± 0.00 mm), and *S. typhi* (10.67 ± 0.57 mm). A further increase in concentration to 100 µL significantly enhanced the antibacterial activity, with *B. subtilis* (26.57 ± 2.37 mm) and *E. coli* (23.57 ± 1.71 mm) showing the highest inhibition, exceeding or approaching the activity of gentamicin. *S. typhi* and *P. vulgaris* also showed marked inhibition zones of 21.86 ± 1.95 mm and 19.86 ± 1.95 mm, respectively.

These results confirm that CoO NPs possess strong antibacterial activity, particularly at higher concentrations, with *B. subtilis* being the most susceptible strain. The enhanced antibacterial effect may be attributed to the nanoscale size, which facilitates penetration through bacterial cell walls, generation of reactive oxygen species (ROS), and disruption of cellular components as depicted in the Fig. 9. The variation in susceptibility among Gram-positive and Gram-negative bacteria suggests that differences in cell wall structure and permeability play a key role in determining nanoparticle efficacy[103–109].

Overall, the findings indicate that biosynthesized CoO NPs exhibit promising broad-spectrum antibacterial potential, comparable to conventional antibiotics, and may serve as alternative antimicrobial agents against multidrug-resistant pathogens. Moreover, the antibacterial activity of nanoparticles can be enhanced by carefully controlling their physical and chemical properties. These factors include particle size, shape, surface area, and crystallinity, which influence how the nanoparticles interact with different cells. Furthermore, phase composition, size distribution, and band gap also play crucial roles in determining their efficacy[110].

Antioxidant activity

The antioxidant potential of *Uraria picta*–mediated cobalt oxide nanoparticles (CoO NPs) was evaluated using the DPPH free radical scavenging assay. The results revealed a dose-dependent response, with the minimum activity recorded as 1.188% inhibition at 5 µg/mL, while the maximum activity reached 8.481% inhibition at 320 µg/mL as depicted in the Fig. 10. These findings indicate that the synthesized CoO NPs exhibit moderate antioxidant activity, as also represented in Table 3 **&** Table 4. The present findings, highlight that phytogenic synthesis not only facilitates eco-friendly production of CoO NPs but also imparts desirable biological properties. While the antioxidant activity of *Uraria picta*–derived CoO NPs appears moderate compared to other reports, their biosynthetic potential and biological efficacy provide a promising foundation for further exploration in therapeutic and biomedical applications (**Fig. S6**).

Conclusion

The present study demonstrates that *Uraria picta* extract functions as an efficient bio-reducing and stabilizing agent for the green synthesis of CoO nanoparticles (CoO NPs) via a simple, non-toxic, and environmentally benign protocol. The synthesized CoO NPs, comprehensively characterized by SEM-EDX, FTIR, HR-TEM, UV–Vis spectroscopy, and XRD analyses, exhibited a globular morphology with an average particle size of 5.257 ± 0.743 nm (minimum 4.010 nm, median 5.395 nm, maximum 6.270 nm), consistent with the reported nanoscale range of 4–5 nm. This green synthesis approach offers a rapid, cost-effective, and sustainable strategy for producing CoO NPs with potential applications in biomedical and industrial sectors. The *Uraria picta*–mediated CoO NPs displayed moderate, dose-dependent antioxidant activity, indicating that phytogenic synthesis confers functional biological properties. Additionally, the nanoparticles exhibited pronounced, concentration-dependent

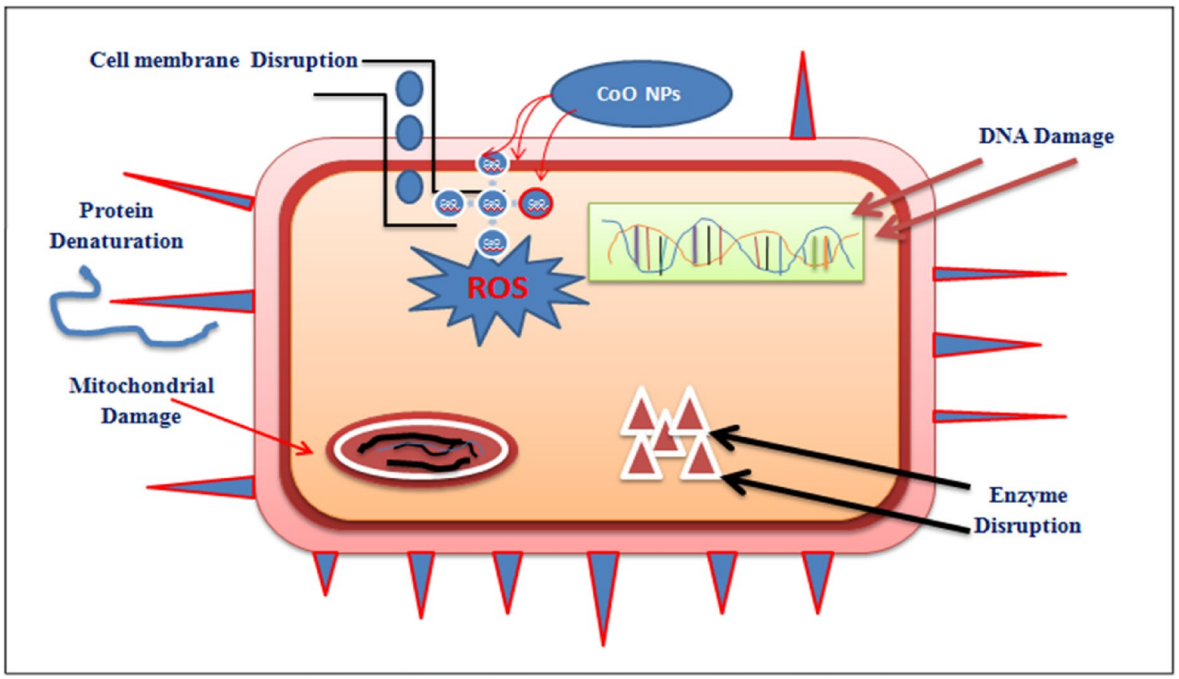

Fig. 9. Proposed mechanisms of CoO NPs against bacterial cell.

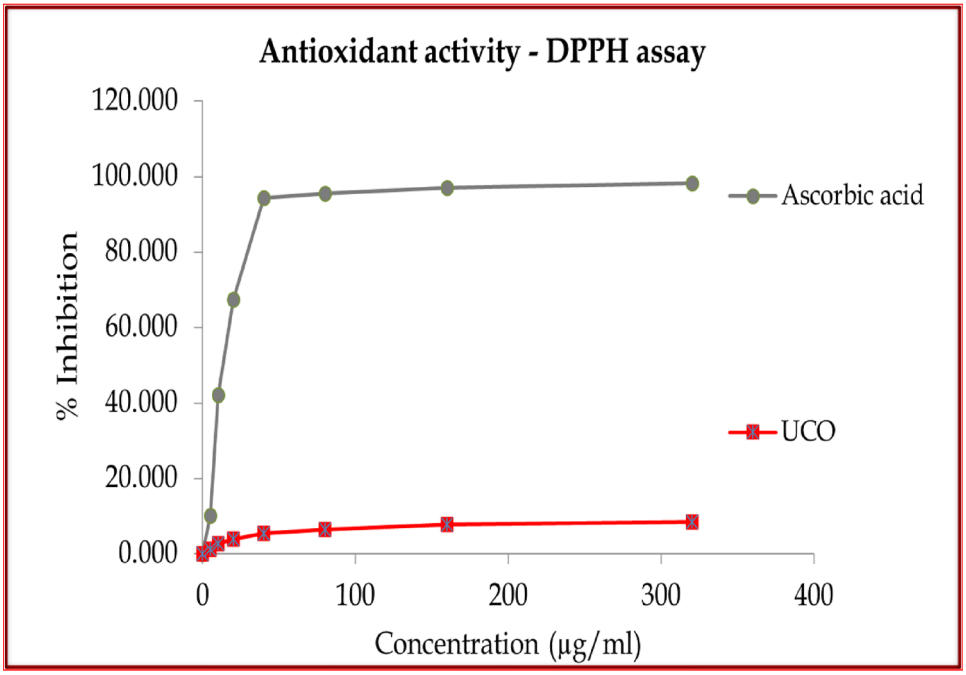

Fig. 10. DPPH based assay profile for ascorbic acid showcasing concentration-based antioxidant activity recorded as IC_{50} value (13.75 µg/mL) and that of *Uraria picta* cobalt oxide NPs with > 320 µg/mL as IC_{50} value.

Experiment Result at 517 nm					% DPPH inhibition					
	Conc. µg/mL	Singlet	Duplicate	Triplicate	Singlet	Duplicate	Triplicate	Mean	SD	IC_{50}µg/mL
Uco	5	0.775	0.771	0.784	1.399	1.658	0.508	1.188	0.604	
	10	0.764	0.763	0.767	2.799	2.679	2.665	2.714	0.074	
	20	0.758	0.753	0.756	3.562	3.954	4.061	3.859	0.263	
	40	0.747	0.744	0.74	4.962	5.102	6.091	5.385	0.616	**> 320**
	80	0.739	0.733	0.736	5.980	6.505	6.599	6.361	0.334	
	160	0.725	0.728	0.722	7.761	7.143	8.376	7.760	0.616	
	320	0.719	0.723	0.716	8.524	7.781	9.137	8.481	0.679	

Table 3. Antioxidant activity of CoO NPs.

Conc. (µg/mL)	% DPPH Inhibition for Ascorbic acid	% DPPH Inhibition for CoO NPs
0	0.000	0.000
5	10.136	1.188
10	42.239	2.714
20	67.387	3.859
40	94.275	5.385
80	95.462	6.361
160	96.989	7.760
320	98.219	8.481

Table 4. Antioxidant activity of nanoparticles via DPPH assay along with standard represents % DPPH inhibition.

antibacterial activity, with *B. subtilis* and *E. coli* demonstrating the highest susceptibility, underscoring their potential as broad-spectrum antimicrobial agents. Collectively, these findings substantiate the utility of *U. picta* in generating biologically active CoO NPs. Future investigations should aim to elucidate the mechanistic role of specific phytochemicals in nanoparticle formation and stabilization, optimize scale-up strategies for industrial

production, and tailor the physicochemical properties of CoO NPs for targeted biomedical applications, including drug delivery, imaging, and antimicrobial interventions.

Data availability

All data generated or analyzed during this study are included within the manuscript and attached supporting file.

Received: 29 August 2025; Accepted: 11 November 2025
Published online: 03 December 2025

References

1. Kumari, S. et al. A comprehensive review on various techniques used for synthesizing nanoparticles. *J. Mater. Res. Technol.* **27**, 1739–1763. https://doi.org/10.1016/j.jmrt.2023.09.291 (2023).
2. Rana, A., Yadav, K. & Jagadevan, S. A comprehensive review on green synthesis of nature-inspired metal nanoparticles: mechanism, application and toxicity. *J. Clean. Prod.* **272**, 122880. https://doi.org/10.1016/j.jclepro.2020.122880 (2020).
3. Naseem, T. & Durrani, T. The role of some important metal oxide nanoparticles for wastewater and antibacterial applications: a review. *Environ. Chem. Ecotoxicol.* **3**, 59–75. https://doi.org/10.1016/j.enceco.2020.12.001 (2021).
4. Arulmurugan, B. et al. Nanostructured metals: opticlectrical, and mechanical properties. In *Mechanics of Nanomaterials and Polymer Nanocomposites* 69–85 (2023). https://doi.org/10.1007/978-981-99-2352-6_4
5. Kumar, S. et al. Optically active nanomaterials and its biosensing applications—a review. *Biosensors* **13**, 85. https://doi.org/10.3390/bios13010085 (2023).
6. Štukovnik, Z., Fuchs-Godec, R. & Bren, U. Nanomaterials and their recent applications in impedimetric biosensing. *Biosensors* **13**, 899. https://doi.org/10.3390/bios13100899 (2023).
7. Malik, S., Muhammad, K. & Waheed, Y. Emerging applications of nanotechnology in healthcare and medicine. *Molecules* **28**, 6624. https://doi.org/10.3390/molecules28186624 (2023).
8. Xia, C. et al. Optimistic and possible contribution of nanomaterial on biomedical applications: a review. *Environ. Res.* **218**, 114921. https://doi.org/10.1016/j.envres.2022.114921 (2023).
9. Chandrasekhar, N. & Vinay, S. P. Yellow colored blooms of *Argemone Mexicana* and *Turnera ulmifolia* mediated synthesis of silver nanoparticles and study of their antibacterial and antioxidant activity. *Appl. Nanosci.* **7**, 851–861. https://doi.org/10.1007/s13204-017-0624-5 (2017).
10. Vinay, S. P., Chandrasekhar, N. & Chandrappa, C. P. Eco-friendly approach for the green synthesis of silver nanoparticles using flower extracts of *Sphagneticola trilobata* and study of antibacterial activity. *Int. J. Pharm. Biol. Sci.* **7**, 145–152 (2017).
11. Jafarzadeh, S. et al. Plant protein-based nanocomposite films: a review on the used nanomaterials, characteristics, and food packaging applications. *Crit. Rev. Food Sci. Nutr.* **63**, 9667–9693. https://doi.org/10.1080/10408398.2022.2070721 (2023).
12. Deshmukh, R. K., Kumar, L. & Gaikwad, K. K. Halloysite nanotubes for food packaging application: a review. *Appl. Clay Sci.* **234**, 106856. https://doi.org/10.1016/j.clay.2023.106856 (2023).
13. Hussein, A. R. et al. Acabamento Antimicrobiano de têxteis a partir Da utilização de nanomateriais. *Braz J. Biol.* **84**, e264947. https://doi.org/10.1590/1519-6984.264947 (2023).
14. Yduzzaman, M., Hassan, A., Anik, H. R., Akter, M. & Islam, M. R. Nanotechnology for high-performance textiles: a promising frontier for innovation. *ChemNanoMat* 9, e202300205 (2023). https://doi.org/10.1002/cnma.202300205
15. Deng, A. et al. Unlocking the potential of MOF-derived carbon-based nanomaterials for water purification through advanced oxidation processes: a comprehensive review on the impact of process parameter modulation. *Sep. Purif. Technol.* **318**, 123998. https://doi.org/10.1016/j.seppur.2023.123998 (2023).
16. Mohamed, H. E. A. et al. Physicochemical and nanomedicine applications of phyto-reduced erbium oxide (Er_2O_3) nanoparticles. *AMB Expr.* **13**, 24. https://doi.org/10.1186/s13568-023-01527-w (2023).
17. Huseien, G. F. Potential applications of core-shell nanoparticles in construction industry revisited. *Appl. Nano*. **4**, 75–114. https://doi.org/10.3390/applnano4020006 (2023).
18. Raj, R. S. et al. Z. Nanomaterials in geopolymer composites: a review. *Dev. Built Environ.* **13**, 100114. https://doi.org/10.1016/j.dibe.2022.100114 (2023).
19. Liu, Y., Zhong, X. & Mohammadian, H. R. Role of carbon nanomaterials in reinforcement of concrete and cement: a new perspective in civil engineering. *Alex Eng. J.* **72**, 649–656. https://doi.org/10.1016/j.aej.2023.04.025 (2023).
20. Hasen, H. M. & Tuama, R. J. Review about the applications of nanoparticles in batteries. *J. Eng.* **29**, 47–60. https://doi.org/10.31026/j.eng.2023.08.04 (2023).
21. Vijayakumar, V. et al. R. 2D layered nanomaterials as fillers in polymer composite electrolytes for lithium batteries. *Adv. Energy Mater.* **13**, 2203326. https://doi.org/10.1002/aenm.202203326 (2023).
22. Gong, Y. & Xue, Y. H. Carbon nanomaterials for stabilizing zinc anodes in zinc-ion batteries. *New. Carbon Mater.* **38**, 438–454. https://doi.org/10.1016/S1872-5805(23)60740-1 (2023).
23. Hussein, H. S. The state of the Art of nanomaterials and its applications in energy saving. *Bull. Natl. Res. Cent.* **47**, 7. https://doi.org/10.1186/s42269-023-00984-4 (2023).
24. Yang, M., Ye, Z., Ren, Y., Farhat, M. & Chen, P. Y. Recent advances in nanomaterials used for wearable electronics. *Micromachines* **14**, 603. https://doi.org/10.3390/mi14030603 (2023).
25. Xu, X. et al. Assembled one-dimensional nanowires for flexible electronic devices via printing and coating: techniques, applications, and perspectives. *Adv. Colloid Interface Sci.* **321**, 102987. https://doi.org/10.1016/j.cis.2023.102987 (2023).
26. Iravani, S. & Varma, R. S. Sustainable synthesis of Cobalt and Cobalt oxide nanoparticles and their catalytic and biomedical applications. *Green. Chem.* **22**, 2643–2661. https://doi.org/10.1039/D0GC00885K (2020).
27. Said, Z. et al. Nanotechnology-integrated phase change material and nanofluids for solar applications as a potential approach for clean energy strategies: progress, challenges, and opportunities. *J. Clean. Prod.* **416**, 137736. https://doi.org/10.1016/j.jclepro.2023.137736 (2023).
28. Wang, Q. et al. A review of applications of plasmonic and conventional nanofluids in solar heat collection. *Appl. Therm. Eng.* **219**, 119476. https://doi.org/10.1016/j.applthermaleng.2022.119476 (2023).
29. Ferry, D. B., Rasheed, T., Anwar, M. T. & Imran, M. Graphene and graphene derived nanomaterials as versatile candidates for organic solar cells and smart windows applications–a review. *ChemistrySelect* **9**, e202301442. https://doi.org/10.1002/slct.202301442 (2024).
30. Hkiri, K., Mohamed, H. E. A., Ghotekar, S. & Maaza, M. Green synthesis of cerium oxide nanoparticles using *Portulaca Oleracea* extract: photocatalytic activities. *Inorg. Chem. Commun.* **162**, 112243. https://doi.org/10.1016/j.inoche.2024.112243 (2024).
31. Mohamed, H. E. A., Hilal-Alnaqbi, A., Dagher, S., Akhozheya, B. & Maaza, M. Green synthesis of $CdWO_4$ nanorods with enhanced photocatalytic activity utilizing hyphaene Thebaica fruit. *ChemistrySelect* **7**, e202201442. https://doi.org/10.1002/slct.202201442 (2022).
32. Omeiza, L. A. et al. Nanostructured electrocatalysts for advanced applications in fuel cells. *Energies* **16**, 1876. https://doi.org/10.3390/en16041876 (2023).

33. Haque, S., Nasar, A., Duteanu, N. & Pandey, S. ul, Carbon-based nanomaterials used in biofuel cells–a review. *Fuel* 331, 125634 (2023). https://doi.org/10.1016/j.fuel.2022.125634
34. Bhatt, R., Shukla, P., Mishra, A. & Bajpai, A. K. Emerging applications of nano-modified bio-fuel cells. *Nanotechnol. Adv. Biofuel.* 213–242. https://doi.org/10.1016/B978-0-323-91759-9.00002-2 (2023).
35. Zhang, D. et al. Recent progress of diversiform humidity sensors based on versatile nanomaterials and their prospective applications. *Nano Res.* **16**, 11938–11958. https://doi.org/10.1007/s12274-022-4917-y (2023).
36. Abedi-Firoozjah, R. et al. Nanomaterial-based sensors for the detection of pathogens and microbial toxins in the food industry: a review on recent progress. *Coord. Chem. Rev.* **500**, 215545. https://doi.org/10.1016/j.ccr.2023.215545 (2024).
37. Lawaniya, S. D. et al. Functional nanomaterials in flexible gas sensors: recent progress and future prospects. *Mater. Today Chem.* **29**, 101428. https://doi.org/10.1016/j.mtchem.2023.101428 (2023).
38. Saleh, T. A. & Fadillah, G. Green synthesis protocols, toxicity, and recent progress in nanomaterial-based environmental chemical sensors applications. *Trends Environ. Anal. Chem.* **39**, e00204. https://doi.org/10.1016/j.teac.2023.e00204 (2023).
39. Ghotekar, S. et al. A novel approach towards biosynthesis of $BiVO_4$ nanoparticles and their anticancer, antioxidant, and photocatalytic activities. *J. Sol-Gel Sci. Technol.* **109**, 784–794. https://doi.org/10.1007/s10971-024-06317-9 (2024).
40. Matussin, S. N. et al. α-Glucosidase inhibitory activity and cytotoxicity of CeO_2 nanoparticles fabricated using a mixture of different cerium precursors. *ACS Omega*. **9**, 157–165. https://doi.org/10.1021/acsomega.3c02524 (2023).
41. El-Khawaga, A. M. & Zidan, A. Abd El-Mageed, A. I. Preparation methods of different nanomaterials for various potential applications: a review. *J. Mol. Struct.* **1281**, 135148. https://doi.org/10.1016/j.molstruc.2023.135148 (2023).
42. Salem, S. S. A mini review on green nanotechnology and its development in biological effects. *Arch. Microbiol.* **205**, 128. https://doi.org/10.1007/s00203-023-03467-2 (2023).
43. Vittaya, L., Chalad, C. & Sirimahachai, U. Green synthesis and biological activities of zinc oxide nanoparticles using ampelocissus martini rhizome extract. *ChemistrySelect* **9**, e202304671. https://doi.org/10.1002/slct.202304671 (2024).
44. Borah, D. et al. Facile green synthesis of highly stable, water dispersible carbohydrate conjugated Ag, Au and Ag–Au biocompatible nanoparticles: catalytic and antimicrobial activity. *Mater. Today Commun.* **37**, 107096. https://doi.org/10.1016/j.mtcomm.2023.107096 (2023).
45. Sheikh, S. et al. Biosynthesis of copper oxide nanoparticles using *Uraria picta* (Jacq.) plant extract and its characterization. *Bioscan* **18**, 29–34 (2025). https://thebioscan.com/index.php/pub/article/view/487
46. Dubadi, R., Huang, S. D. & Jaroniec, M. Mechanochemical synthesis of nanoparticles for potential antimicrobial applications. *Materials* **16**, 1460. https://doi.org/10.3390/ma16041460 (2023).
47. Mali, S. C., Dhaka, A., Sharma, S. & Trivedi, R. Review on biogenic synthesis of copper nanoparticles and its potential applications. *Inorg. Chem. Commun.* **149**, 110448. https://doi.org/10.1016/j.inoche.2023.110448 (2023).
48. Nguyen, D. T. C. et al. New frontiers of invasive plants for biosynthesis of nanoparticles towards biomedical applications: a review. *Sci. Total Environ.* **857**, 159278. https://doi.org/10.1016/j.scitotenv.2022.159278 (2023).
49. Singh, J., Kaur, G. & Rawat, M. A brief review on synthesis and characterization of copper oxide nanoparticles and its applications. *J. Bioelectron. Nanotechnol.* **1**, 9 (2016).
50. Raman, V. et al. Synthesis of Co_3O_4 nanoparticles with block and sphere morphology, and investigation into the influence of morphology on biological toxicity. *Exp. Ther. Med.* **11**, 553–560. https://doi.org/10.3892/etm.2015.2946 (2016).
51. Khalil, A. T. et al. Biosynthesis of iron oxide (Fe_2O_3) nanoparticles via aqueous extracts of *Sageretia thea* (Osbeck) and their pharmacognostic properties. *Green. Chem. Lett. Rev.* **10**, 186–201. https://doi.org/10.1080/17518253.2017.1339831 (2017).
52. Singh, A. K. A review on plant extract-based route for synthesis of Cobalt nanoparticles: photocatalytic, electrochemical sensing and antibacterial applications. *Curr. Res. Green. Sustain. Chem.* **5**, 100270. https://doi.org/10.1016/j.crgsc.2022.100270 (2022).
53. Diallo, A., Beye, A. C., Doyle, T. B., Park, E. & Maaza, M. Green synthesis of Co_3O_4 nanoparticles via *Aspalathus linearis*: physical properties. *Green. Chem. Lett. Rev.* **8**, 30–36. https://doi.org/10.1080/17518253.2015.1082646 (2015).
54. Askarinejad, A., Bagherzadeh, M. & Morsali, A. Catalytic performance of Mn_3O_4 and Co_3O_4 nanocrystals prepared by sonochemical method in epoxidation of styrene and cyclooctene. *Appl. Surf. Sci.* **256**, 6678–6682. https://doi.org/10.1016/j.apsusc.2010.04.069 (2010).
55. Kaviyarasu, K., Raja, A. & Devarajan, P. A. Structural Elucidation and spectral characterizations of Co_3O_4 nanoflakes. *Spectrochim Acta Mol. Biomol. Spectrosc.* **114**, 586–591. https://doi.org/10.1016/j.saa.2013.04.126 (2013).
56. Akhlaghi, N., Najafpour-Darzi, G. & Younesi, H. Facile and green synthesis of Cobalt oxide nanoparticles using ethanolic extract of *Trigonella foenum-graecum* (Fenugreek) leaves. *Adv. Powder Technol.* **31**, 3562–3569. https://doi.org/10.1016/j.apt.2020.07.004 (2020).
57. Asha, G., Rajeshwari, V., Stephen, G., Gurusamy, S. & D. RachelC. J. Eco-friendly synthesis and characterization of Cobalt oxide nanoparticles by allium sativum species and its photocatalytic activity. *Mater. Today Proc.* **48**, 486–493. https://doi.org/10.1016/j.matpr.2021.02.338 (2022).
58. Gaikar, P. S. et al. Green synthesis of Cobalt oxide thin films as an electrode material for electrochemical capacitor application. *Curr. Res. Green. Sustain. Chem.* **5**, 100265. https://doi.org/10.1016/j.crgsc.2022.100265 (2022).
59. Chattopadhyay, S. et al. Surface-modified Cobalt oxide nanoparticles: new opportunities for anti-cancer drug development. *Cancer Nanotechnol.* **3**, 13–23. https://doi.org/10.1007/s12645-012-0026-z (2012).
60. Khalil, A. T. et al. Physical properties, biological applications and biocompatibility studies on biosynthesized single phase Cobalt oxide (Co_3O_4) nanoparticles via *Sageretia thea* (Osbeck). *Arab. J. Chem.* **13**, 606–619. https://doi.org/10.1016/j.arabjc.2017.07.004 (2020).
61. Ajarem, J. S., Maodaa, S. N., Allam, A. A., Taher, M. M. & Khalaf, M. Benign synthesis of Cobalt oxide nanoparticles containing red algae extract: antioxidant, antimicrobial, anticancer, and anticoagulant activity. *J. Clust Sci.* **33**, 717–728. https://doi.org/10.1007/s10876-021-02004-9 (2022).
62. Rasheed, T., Nabeel, F., Bilal, M. & Iqbal, H. M. Biogenic synthesis and characterization of Cobalt oxide nanoparticles for catalytic reduction of direct yellow-142 and Methyl orange dyes. *Biocatal. Agric. Biotechnol.* **19**, 101154. https://doi.org/10.1016/j.bcab.2019.101154 (2019).
63. Iqbal, J. et al. Biogenic synthesis of green and cost-effective Cobalt oxide nanoparticles using *Geranium Wallichianum* leaves extract and evaluation of in vitro antioxidant, antimicrobial, cytotoxic and enzyme Inhibition properties. *Mater. Res. Express*. **6**, 115407. https://doi.org/10.1088/2053-1591/ab4f04 (2019).
64. Hou, H. et al. Retracted article: novel green synthesis and antioxidant, cytotoxicity, antimicrobial, antidiabetic, anticholinergics, and wound healing properties of Cobalt nanoparticles containing *Ziziphora clinopodioides* lam leaves extract. *Sci. Rep.* **10**, 12195. https://doi.org/10.1038/s41598-020-68951-x (2020).
65. Momen Eslamiehei, F., Mashreghi, M. & Matin, M. M. Advancing colorectal cancer therapy with biosynthesized Cobalt oxide nanoparticles: a study on their antioxidant, antibacterial, and anticancer efficacy. *Cancer Nanotechnol.* **15**, 22. https://doi.org/10.1186/s12645-024-00258-2 (2024).
66. Bhusare, B. P., Ahire, M. L., John, C. K. & Nikam, T. D. *Uraria picta*: a comprehensive review on evidences of utilization and strategies of conservation. *J. Phytol.* **13**, 41–47. https://doi.org/10.25081/jp.2021.v13.7028 (2021).
67. Ved, D. K. & Goraya, G. S. Demand and supply of medicinal plants in India. *NMPB FRLHT*. **18** (85), 210–252 (2007).
68. Vats, S., Kaushal, C., Timko, M. P. & Ganie, S. A. *Uraria picta*: a review on its ethnobotany, bioactive compounds, Pharmacology and commercial relevance. *S Afr. J. Bot.* **167**, 333–354. https://doi.org/10.1016/j.sajb.2024.02.008 (2024).

69. Rahman, M. M., Gibbons, S. & Gray, A. I. Isoflavanones from *Uraria picta* and their antimicrobial activity. *Phytochemistry* **68**, 1692–1697. https://doi.org/10.1016/j.phytochem.2007.04.015 (2007).
70. Chole, P. & Manjunath, B. T. Green synthesis of cobalt oxide nanoparticles with *in vitro* cytotoxicity assessment using *pomegranate* (*Punica granatum* L.) seed oil: a promising approach for antimicrobial and anticancer applications. *Pharm. Sci. Technol.* 11, e (2024). (2024) https://doi.org/10.14719/pst.2024.11.2
71. Mane, J. A., Nagore, D. H. & Chitlange, S. O. *Uraria picta* (Jacq.): a review on ethnomedical uses, phytochemistry, and biological activities. *Asian J. Pharm. Clin. Res.* **14**, 40–44. https://doi.org/10.22159/ajpcr.2021v14i3.40383 (2021).
72. Mohamed, H. Optical properties of bio-engineered nano-scaled Y_2O_3 particles via *Hyphaene Thebaica* natural extract. *J. Phys. Conf. Ser.* **2970**, 012003. https://doi.org/10.1088/1742-6596/2970/1/012003 (2025).
73. Akash, M. S. H. & Rehman, K. *Essentials of Pharmaceutical Analysis* 167–174 (Springer, 2020). https://doi.org/10.1007/978-981-15-2098-0
74. Kalsi, P. S. *Spectroscopy of Organic Compounds* (New Age International, 2007).
75. Wang, Z. L. New developments in transmission electron microscopy for nanotechnology. *Adv. Mater.* **15**, 1497–1514. https://doi.org/10.1002/adma.200300384 (2003).
76. Fultz, B. & Howe, J. M. *Transmission Electron Microscopy and Diffractometry of Materials* (Springer, 2008). https://doi.org/10.1007/978-3-540-73886-2_7
77. Thomson, L., Saiju, A., Femina, C., Ph, D. & Dissertation St. Teresa's College, Ernakulam (2019).
78. Bertolotti, F., Moscheni, D., Guagliardi, A. & Masciocchi, N. When crystals go nano: the role of advanced X-ray total scattering methods in nanotechnology. *Eur. J. Inorg. Chem.* 3789–3803. https://doi.org/10.1002/ejic.201800534 (2018).
79. Perez, C. Antibiotic assay by agar-well diffusion method. *Acta Biol. Med. Exp.* **15**, 113–115 (1990).
80. Warrier, P. K. *Indian Medicinal Plants: A Compendium of 500 Species*, Vol. 5Orient Blackswan, (1993).
81. Harborne, A. J. *Phytochemical Methods: A Guide To Modern Techniques of Plant Analysis* (Springer Science & Business Media, 1998).
82. Ghosh, K., Rawal, P. & Pramanik, S. *Vivo* antioxidant and hypoglycaemic potentials of *Rivina humilis* extract against streptozotocin-induced diabetes and its complications in *Wistar* rats. *J. Diabetes Metab. Disord.* **22**, 1373–1383. https://doi.org/10.1007/s40200-023-01258-6 (2023).
83. Perumal, V. & Ilangkumaran, M. The influence of copper oxide nanoparticle added *Pongamia* Methyl ester biodiesel on the performance, combustion and emission of a diesel engine. *Fuel* **232**, 791–802. https://doi.org/10.1016/j.fuel.2018.04.129 (2018).
84. Mane, P. C. et al. Green adeptness in synthesis of non-toxic copper and Cobalt oxide nanocomposites with multifaceted bioactivities. *Cancer Nanotechnol.* **14**, 79. https://doi.org/10.1186/s12645-023-00226-2 (2023).
85. Singh, J., Mehta, A., Rawat, M., Basu, S. & Chandel, S. *Allium sativum*–mediated phytogenic synthesis of Cobalt oxide nanoparticles and their antibacterial potential. *Appl. Nanosci.* **11**, 2807–2817. https://doi.org/10.1007/s13204-020-01513-0 (2021).
86. Sahoo, S. K., Parida, U. K., Nayak, P. L., Nayak, S. & Panda, S. Green synthesis of Cobalt oxide nanoparticles using *Hibiscus rosa-sinensis* and its antimicrobial activity. *Asian J. Chem.* **27**, 3453–3456. https://doi.org/10.14233/ajchem.2015.18674 (2015).
87. Asha, G., Rajeshwari, V., Stephen, G., Gurusamy, S. & Rachel, D. C. J. Eco-friendly synthesis and characterization of cobalt oxide nanoparticles and its photocatalytic activity. *Mater. Today Proc.* 48, 486–493 (2022). https://doi.org/10.3390/w15050910
88. Govindasamy, R. et al. Green synthesis and characterization of Cobalt oxide nanoparticles using *Psidium Guajava* leaves extracts and their photocatalytic and biological activities. *Molecules* **27**, 5646. https://doi.org/10.3390/molecules27175646 (2022).
89. Abdi, M., Yusuf, Z. & Sasikumar, J. M. Phyto-fabrication of Cobalt oxide nanoparticles from *Ocimum gratissimum* L. leaf and flower extracts and their antimicrobial activities. *Open. Biotechnol. J.* **17**, 1–10. https://doi.org/10.2174/0118740707261876230919053208 (2023).
90. Hemalatha, M. et al. Application of green synthesized ag and Cu nanoparticles for the control of bruchids and their impact on seed quality and yield in Greengram. *Heliyon* **10**, e31551. https://doi.org/10.1016/j.heliyon.2024.e31551 (2024).
91. Al-Qasmi, N. Sustainable and efficacy approach of green synthesized Cobalt oxide (Co_3O_4) nanoparticles and evaluation of their cytotoxicity activity on cancerous cells. *Molecules* **27**, 8163. https://doi.org/10.3390/molecules27238163 (2022).
92. Mubraiz, N., Bano, A., Mahmood, T. & Khan, N. Microbial and plant-assisted synthesis of Cobalt oxide nanoparticles and their antimicrobial activities. *Agronomy* **11**, 1607. https://doi.org/10.3390/agronomy11081607 (2021).
93. Kgosiemang, I. K. et al. Green synthesis of magnesium and Cobalt oxide nanoparticles using *Euphorbia tirucalli*: characterization and potential application for breast cancer Inhibition. *Inorg. Nano-Met Chem.* **50**, 1070–1080. https://doi.org/10.1080/24701556.2020.1735422 (2020).
94. Moawad, R. et al. Biosynthesis and health-promoting traits of green synthesized Cobalt oxide nanoparticles. *Sci. Rep.* **15**, 727. https://doi.org/10.1038/s41598-024-82679-y (2025).
95. Matyi, R. J. & MacCuspie, R. I. *IEEE Nanotechnol Mag* **14**, 1–12 (2020).
96. Khodaei, M. & Petaccia, L. (eds) *X-ray Characterization of Nanostructured Energy Materials by Synchrotron Radiation* (BoD–Books on Demand, 2017).
97. Masadeh, S. et al. *Phys. Rev. B* **76**, 1–10 (2007).
98. Honkeldieva, M. T., Li, H., Bukhorov, K. X., Ahmedov, H. A. & Yulbarsova, M. V. Fourier transformation of infrared spectroscopy and X-ray diffraction analyses of NPK mineral and biomineral fertilizers. *IOP Conf. Ser. : Earth Environ. Sci.* **868**, 012042. https://doi.org/10.1088/1755-1315/868/1/012042 (2021).
99. Manikandan, R. et al. Eco-friendly synthesis, spectral, morphological analysis of Cobalt oxide nanoparticles (Co_3O_4NPs) mediated by leaves extract of *Pedalium murex* L. and its antibacterial, antifungal, antioxidant and anticancer (MCF-7 cell line) study. *Indian J. Sci. Technol.* **18**, 102–112. https://doi.org/10.17485/IJST/v18i2.2816 (2025).
100. Ogunyemi, S. O. et al. Cobalt oxide nanoparticles: an effective growth promoter of *Arabidopsis* plants and nano-pesticide against bacterial leaf blight pathogen in rice. *Ecotoxicol. Environ. Saf.* **257**, 114935. https://doi.org/10.1016/j.ecoenv.2023.114935 (2023).
101. Ghodake, G., Seo, Y. D. & Lee, D. S. Hazardous phytotoxic nature of Cobalt and zinc oxide nanoparticles assessed using *Allium Cepa*. *J. Hazard. Mater.* **186**, 952–955. https://doi.org/10.1016/j.jhazmat.2010.11.039 (2011).
102. Raeisi, M. et al. Magnetic Cobalt oxide nanosheets: green synthesis and *in vitro* cytotoxicity. *Bioprocess. Biosyst Eng.* **44**, 1423–1432. https://doi.org/10.1007/s00449-021-02518-6 (2021).
103. Aldeen, T. S., Mohamed, H. E. A. & Maaza, M. ZnO nanoparticles prepared via a green synthesis approach: physical properties, photocatalytic and antibacterial activity. *J. Phys. Chem. Solids*. **160**, 110313. https://doi.org/10.1016/j.jpcs.2021.110313 (2022).
104. Vinay, S. P., Udayabhanu, U. & Lalithamba, H. S. Plant-mediated green synthesis of ag nanoparticles using *Rauvolfia tetraphylla* (L.) flower extracts: characterization, biological activities, and screening of the catalytic activity in formylation reaction. *Sci. Iran.* **27**, 3353–3366. https://doi.org/10.24200/sci.2019.51275.2093 (2020).
105. Pawar, A., Mungole, A. & Naktode, K. Biosynthesis of CuO nanoparticles using plant extract as a precursor: characterization, antibacterial, and antioxidant activity. *Nano Biomed. Eng.* **15** https://doi.org/10.26599/NBE.2023.9290027 (2023). [Article ID not provided].
106. Pawar, A., Mungole, A. & Naktode, K. Biogenic copper oxide nanoparticles synthesized from whole plant extract of *Nicotiana Plumbaginifolia* Viv.: characterization, antibacterial, and antioxidant properties. *J. Turk. Chem. Soc. A: Chem.* **11**, 1005–1016. https://doi.org/10.18596/jotcsa.1422924 (2024).
107. Sheikh, S. et al. Greener synthesis of copper oxide nanoparticles using Rivina humilis L. plant extract, characterization and their biological evaluation for antimicrobial and antioxidant activity. *ChemSelect* **9** (e202401219). https://doi.org/10.1002/slct.202401219 (2024).

108. Pandhurnekar, C. P., Pandhurnekar, H. C., Yadao, B. G., Mungole, A. J. & Mohabe, P. Recent advances in rare earth metal-doped nanomaterials and their applications in biomedical imaging techniques. *AIP Conf. Proc.* 2974, 020044 (2024). https://doi.org/10.1063/5.0181801
109. Mungole, A. J. et al. Biological synthesis of silver nanoparticles for antimicrobial applications: a short review. *J. Adv. Sci. Res* **12**, 7–10 (2021).
110. Vinay, S. P., Udayabhanu, G., Chandrappa, C. P. & Chandrasekhar, N. Enhanced photocatalysis, photoluminescence, and antibacterial activities of nanosized ag: green synthesized via *Rauvolfia tetraphylla* (devil pepper). *SN Appl. Sci.* **1**, 477. https://doi.org/10.1007/s42452-019-0437-0 (2019).

Acknowledgements
We would like to thank Principal, N. H. College, Bramhapuri, Maharashtra (India) for their support, motivation, and providing facilities for the execution of this work. Also, thanks to SAIF, Cochin, for the characterization of samples. The authors would also like to thank the Ongoing Research Funding Program (ORF-2025-1042), King Saud University, Riyadh, Saudi Arabia.

Author contributions
S.S.: Writing - Original Draft; A.J.M.: Methodology, Visualization and Experimental design; A.R.B. Project administration; A.P.P.: Conceptualization; C.P.P.: Methodology; H.C.P.: Data Curation & Biological activities; R.W.: Funding acquisition; H.P.K.: Validation; V.J.U.: Validation & Investigation; S.A.: Writing – Review, Editing & submission; D.M.P.: Result interpretation; M.A-O.: Formal analysis; P.E.: Review & Editing Manuscript.

Funding
King Saud University, Riyadh, Saudi Arabia, Ongoing Research Funding Program (ORF-2025-1042) and Parul Institute of Applied Sciences (PIAS), Parul University, PO Limda, Tal Waghodia – 391 760, India.

Declarations

Consent for publication
All of the authors consent to publish this work.

Competing interests
The authors declare no competing interests.

Conflict of interest
On behalf of all authors, the corresponding authors states that there is no conflict of interest.

Declaration of competing interest
There are no pertinent financial or non-financial interests that the authors need to disclose.

Consent to participate
All of the authors consent to participate in this research work.

Ethical approval
The collection of plants for this experimental research exploration are in strict agreement with relevant national, international, and institutional regulations and guidelines and complies with the IUCN Policy Statement on Research Involving Species at Risk of Extinction and the Convention on the Trade in Endangered Species of Wild Fauna and Flora. We also declare herein that our paper is original and unpublished elsewhere and that this manuscript complies to the Ethical Rules applicable for this journal.

Additional information
Supplementary Information The online version contains supplementary material available at https://doi.org/10.1038/s41598-025-28596-0.

Correspondence and requests for materials should be addressed to A.J.M., A.R.B., V.J.U. or S.A.